IOP Conference Series: Materials Science and Engineering

PAPER • OPEN ACCESS

Determination of Temperature Rise and Temperature Differentials of CEMII/B-V Cement for 20MPa Mass Concrete using Adiabatic Temperature Rise Data

To cite this article: GO Chee Siang 2017 *IOP Conf. Ser.: Mater. Sci. Eng.* **217** 012008

View the article online for updates and enhancements.

You may also like

- Characteristics of the spatiotemporal distribution of daily extreme temperature events in China: Minimum temperature records in different climate states against the background of the most probable temperature
Zhong-Hua Qian, , Jing-Guo Hu et al.
- Suggestion models of temperature differentials for the composite box girder bridge
Hesham A Numan, Heba Kadhm Salman, Aamer N Abbas et al.
- A wide range temperature controller using a resistance element
S J Borgars

This content was downloaded from IP address 176.88.22.162 on 08/02/2024 at 09:23

IOP Conf. Series: Materials Science and Engineering **217** (2017) 012008 doi:10.1088/1757-899X/217/1/012008

Determination of Temperature Rise and Temperature Differentials of CEMII/B-V Cement for 20MPa Mass Concrete using Adiabatic Temperature Rise Data

GO Chee Siang

30, Jalan 1/27D, Seksyen 6, Wangsa Maju 53300, Kuala Lumpur, West Malaysia.

csgo@loh-loh.com.my

Abstract. Experimental test was carried out to determine the temperature rise characteristics of Portland-Fly-Ash Cement (CEM II/B-V, 42.5N) of Blaine fineness 418.6m^2/kg and 444.6m^2/kg respectively for 20MPa mass concrete under adiabatic condition. The estimation on adiabatic temperature rise by way of CIRIA C660 method (Construction Industry Research & Information Information) was adopted to verify and validate the hot-box test results by simulating the heat generation curve of the concrete under semi-adiabatic condition. Test result found that Portland fly-ash cement has exhibited decrease in the peak value of temperature rise and maximum temperature rise rate. The result showed that the temperature development and distribution profile, which is directly contributed from the heat of hydration of cement with time, is affected by the insulation, initial placing temperature, geometry and size of concrete mass.

The mock up data showing the measured temperature differential is significantly lower than the technical specifications 20°C temperature differential requirement and the 27.7°C limiting temperature differential for granite aggregate concrete as stipulated in BS8110-2: 1985. The concrete strength test result revealed that the 28 days cubes compressive strength was above the stipulated 20MPa characteristic strength at 90 days. The test demonstrated that with proper concrete mix design, the use of Portland flyash cement, combination of chilled water and flake ice, and good insulation is effective in reducing peak temperature rise, temperature differential, and lower adiabatic temperature rise for mass concrete pours. As far as the determined adiabatic temperature rise result was concern, the established result could be inferred for in-situ thermal properties of 20MPa mass concrete application, as the result could be repeatable on account of similar type of constituent materials and concrete mix design adopted for permanent works at project site.

Keywords: Mass concrete, Portland-fly-ash cement (CEM II/B-V), Initial placing temperature, Heat of hydration, Adiabatic temperature rise, Peak temperature, Temperature differential, Compressive strength.

1. INTRODUCTION

In large concrete elements, the interior is considered to be hydrating in an essentially adiabatic process. Because of the low thermal conductivity of concrete, the heat of hydration from its interior is prevented from being released into the environment, thus a negligible amount of heat is lost, compare to exterior of concrete element. The resulting large temperature differential between the interior and exterior of a concrete element may lead to thermal cracking.

Content from this work may be used under the terms of the Creative Commons Attribution 3.0 licence. Any further distribution of this work must maintain attribution to the author(s) and the title of the work, journal citation and DOI.
Published under licence by IOP Publishing Ltd

The term adiabatic refers to a process occurring without the gain or loss of heat. Adiabatic temperature measurement is used to simulate the condition in the interior of a large concrete element so that the maximum heat development potential in any concrete mix can be measured (Lee MH, Khil BS & Yun HD 2014). This data may then be used as input parameter for subsequent thermal modelling in the pursuit to determine the risk level and thermal cracking potential. Owing to data of this kind is not available locally; therefore adiabatic temperature rise test was carried out to determine the peak concrete core temperature, temperature differential and temperature gradient for this 20MPa mass concrete. This was determined through trial hot-box tests at prescribed initial placing temperature and anticipated concrete section thickness, rather than merely follow project contract specifications requirements (Technical Specifications 2000; 2007; 2009, 2010 & 2013), as stipulated below:

(1) The fresh concrete placing temperature shall not exceeding 20°C;
(2) Maximum core-surface temperature differential shall not exceeding 20°C

To avoid surface cracking caused by heat generated in the concrete, European Standard ENV 206: 1992 suggests that the limit on the temperature differential between core and surface is 20°C and the average maximum temperature limit of concrete at core is 60°C. Based on UK experience (BS 8110-2: 1985), by limiting temperature differential to 20°C in *gravel* aggregate concrete, cracking can be avoided. This represents an equivalent restraint factor R of 0.36. However, MS523-2: 2011, Clause A9.3 has specified peak placing temperature of 30°C for mass concrete structure construction. As for the case of HTP project, the proposed quarried rocks for mass concrete production was *granite* aggregate whereby the limiting temperature differential adopted should be capped at 27.7°C instead of 20°C; BS 8110-2: 1985 (pp. 32), Table 3.2- Estimated limiting temperature changes to avoid cracking has specified that limiting temperature differential when R = 0.36 is 27.7°C when granite aggregate concrete was adopted for mass concrete production and construction. However, BS 8110-2: 1985 does not specify the fresh concrete placing temperature and peak temperature requirements in tropical environment.

Concrete temperature rise test under adiabatic condition is normally an approach in laboratory to evaluate the exothermic characteristics of the hydration of the concrete. In this case, 20MPa plain concrete trial hot-box with an array of thermocouples and strain gauges are used to assess the characteristics of the temperature rise, maximum temperature difference and temperature distribution profile in mass concrete were conducted with due consideration given on the selection of concrete block size and geometry, insulation, thermal couples and strain gauges locations, and the duration of temperature monitoring. Due to the reduced rate of hydration, the use of CEMII/B-V cement to replace OPC (CEM 1) is one of the recommended practices to considerably reduce the temperature rise in mass concrete. Since hydration occurs at the surface of cement particles, therefore finely ground cement will have a higher rate of hydration. As finely ground cement has a higher specific surface area, which means there is more area in contact with water for more complete hydration. The finer particles will also be more fully hydrated then coarser particles. However, the total heat of hydration at very late ages is not significantly affected.

This research is intended to overcome the above-mentioned 20MPa mass concrete specification requirements for the construction of Tembat Hydropower dam by adopting more prudent temperature control requirements through subsequent thermal modelling rather than arbitrary determined basing on designer's temperate country experience and practices, which is overly conservative, costly method, and non-sustainable due to carbon emission by running huge capacity of chillers and flake-ice plant to bring down the temperature of water for making concrete and aggregates substantially.

The experimental program was carried out in accordance with the procedure as shown in below Table 1. This experiment is to determine the temperature rise characteristics of Portland-fly-ash cement concrete under adiabatic conditions as well as the compliance to 20MPa characteristic strength

in 90 days. The established adiabatic temperature rise test results (Adiabatic Temperature Rise Test Results 2011 & 2012) allow better understanding of the temperature rise characteristics and its time-base temperature distribution profiles in the mass concrete, whereby the establish result could be adopted as input parameter for subsequent thermal simulation purposes.

Table 1. Procedure for Adiabatic Temperature Rise Modelling Test

Step:	Procedure
1	Analysis of raw material test results, i.e. cementitious, aggregates, admixtures, water for making concrete (similar to site material) and etc, complying with HTP project technical specifications and/or equivalent international codes and standards prior to Hot-Block casting and testing.
2	Key material selection and factors affecting the temperature rise as per "ACI305R-99 on Hot Weather Concreting" and temperature distribution profile in mass concrete.
3	Establishment of concrete mix design and concrete production for 20MPa Class A mass concrete.
4	Casting of Hot-Block using raw materials established from step 1 above
5	Temperature probing, slump measurements and concrete sampling using cube and cylinders as per testing plan carried out by established and accredidated testing laboratory.
6	Adiabatic temperature rise monitoring tests:
	(i) March 2011: 12 days; (ii) June 2012 : 15 days.
7	Compilation of testing results and data analysis.
8	Temperature analysis and interpretation of results.
9	Conclusions/Recommendations

2. EXPERIMENTAL SET-UP

For Stage 1 testing, two (2) hot boxes were prepared as part of the trials. The first hot box (HB1) was prepared with full insulation (100mm thick MRB-32 Insulation Board) with block size of dimension 1.5m x 1.5m x 1.5m and two sets of thermocouples (thermocouples wire type K) installed, one set (3 thermocouple each) at the center and the other set (3 thermocouple each) at the corner of the hot-box and two strain gauges installed at the centre of the block. A second hot block (HB2) of dimension of 1.3m x 1.3m x 1.3m was prepared with two sets of thermocouples installed, one set (3 thermocouple each) at the center and the other set (3 thermocouple each) at the corner of the block. In this case, the base and sides were insulated but the top surface of the box was exposed to the environment. Based on the completed trials conducted on 11/2/2011 and 12/2/2011, an identical concrete mix design was selected for the hot box casting as given in Table 5 (see Page 3 of 11). For stage 2 testing, one hot box was prepared at Hulu Terengganu project site with similar block size and configuration with stage 1 HB, comply with full insulation (100mm thick MRB-32 insulation Board) and two sets each of thermocouples and strain gauges installed using identical concrete mix design as indicated in Table 3.3, whereby the trial was conducted on 21/6/2012.

2.1 Test Specimen

For the evaluation of the temperature rise in mass concrete trial block, a 1.5m x 1.5m x 1.5m concrete block was cast. Blended cement (CEM II/ B-V) containing 25% fly ash was used for the Grade 20 mass concrete hot block trial. The cement content and water/cement ratio was 200 kg/m3 and 0.70 (Stage 1 & 2), respectively. The schematic drawing of the block is described in Figures 1-3, with the locations of the thermocouples, 100mm insulation and timber formwork indicated. 100mm thick MRB-32 insulation board was adopted as the insulation to the concrete mass around the six sides. The top of the concrete was only covered with the polyfoam. Tc is the core temperature at center of the block while Ts and Tn represent the temperature at surface and corner location as indicated in the schematic drawing. The peak core temperatures obtained from stage 1-HB1, stage 1-HB2 and stage 2-HB1 were also used to determine the repeatability of the experiments.

2.2 Equipment

(i) Thermocouple wires Type K manufactured by Tokyo Sokki Kenkyujo Co. Ltd of Japan, and vinyl insulated 0.32 x 1p K-G, with 20mm diameter protective PVC pipe for thermocouples wires.
(ii) Vibrating Wire Embedment Strain Gauge [VWSG] (Model: 5265099)
(iii) Data-logger model CR10X from Campbell Scientific Inc
(iv) AM 16/32multiplexer for multiple data input from Campbell Scientific Inc
(v) VWSG interface module, AVWI and Laptops.

2.3 Casting of Hot-Box

Hot-box is casted with 20Mpa temperature control concrete (average 25°C) with MSA 75mm whereby compaction was done by using 50mm vibrator pokers.

2.4 Data Acquisition

Campbell scientific CR10X data-logger was program automatically to record concrete temperature (°C) and VWSG's strain (με) data at every hourly interval simultaneously for a period of 7 days and the data are downloaded to laptop. The maximum temperature is defines as the readings when no further appreciably rise in temperature over a period of 3 – 4 successive hours).

3. CONCRETE MIX DESIGN AND STRENGTH ANALYSIS

The physical properties and chemical compositions as well as the fineness of the Portland-fly-ash cement (PFAC) used in the study are shown in Tables 2-4 respectively. Table 5 presents the concrete mix design for grade 20 mass concrete applications for all three concrete hot-box tests. The measured initial placing temperature of the mixes was 23°C to 25°C respectively.

Table 2. Typical physical properties of PFA Cement (CIMA, 2011 & 2012)

PFAC (CEM II/B-V)	
Standard	EN197-1 – CEM II/B – V 42.5N – LH
Typical Properties	
Blaine fineness (m^2/kg)	420
Specific gravity	2.9
Initial Setting time (min.)	157
2d strength (MPa)	22
7d strength (MPa)	37
28d strength (MPa)	50

Table 3. Typical chemical analysis of PFA cement (CIMA, 2011& 2012)

Chemical Properties	Chemical Composition (%)
SiO_2	26.57
Al_2O_3	8.84
Fe_2O_3	5.40
CaO	51.89
MgO	0.63
SO_3	2.31
Na2O	0.18
K2O	0.72
Na2O + 0.658 x K2O	0.65
Cl-	0.009

Table 4. Cement test result on properties of specific surface area and heat of hydration (CIMA, 2011 & 2012)

Issue Date	Blaine (cm^2/g)	Heat of Hydration @7D, 270 Max (J/g)
Jan 2011	4186	258
June 2012	4446	274

Table 5. Class A mass concrete C20 mix design (Mass Concrete Class A, 2011)

Description	Value
Cement (kg/m^3)	200
Water (kg/m^3)	140
Sand (kg/m^3)	756
Coarse Aggregate (20mm) (kg/m^3)	1287
Realset 233 (l/m^3)	1.6
Realflow 610 (l/m^3)	0.8
Slump (mm)	20-50
Characteristic Strength (MPa)	20
S/A Ratio (Sand/ Aggregates)	0.37
W/C Ratio(Water/Cement)	0.70

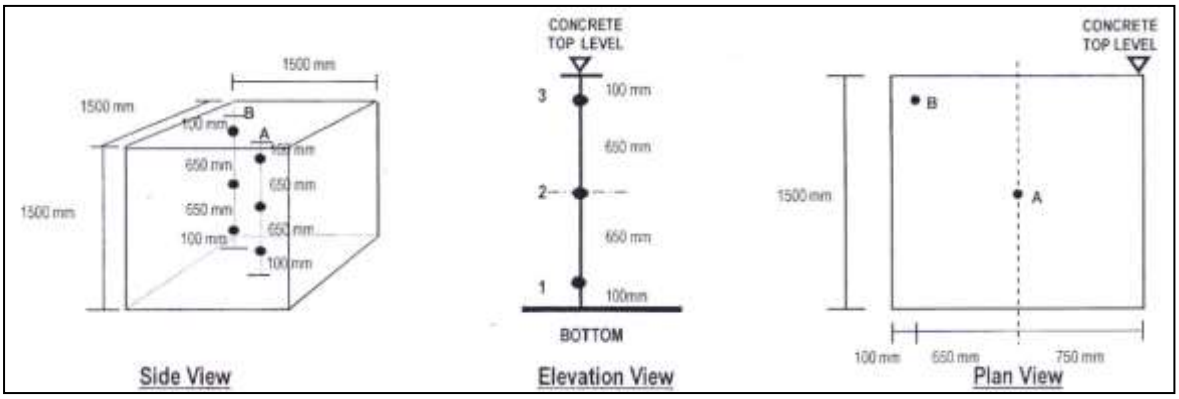

Figure 1. Sketch showing locations of thermocouples in 1.5m x 1.5m x 1.5m hot-box for Stage 1-HB1 and Stage 2-HB1 m^3

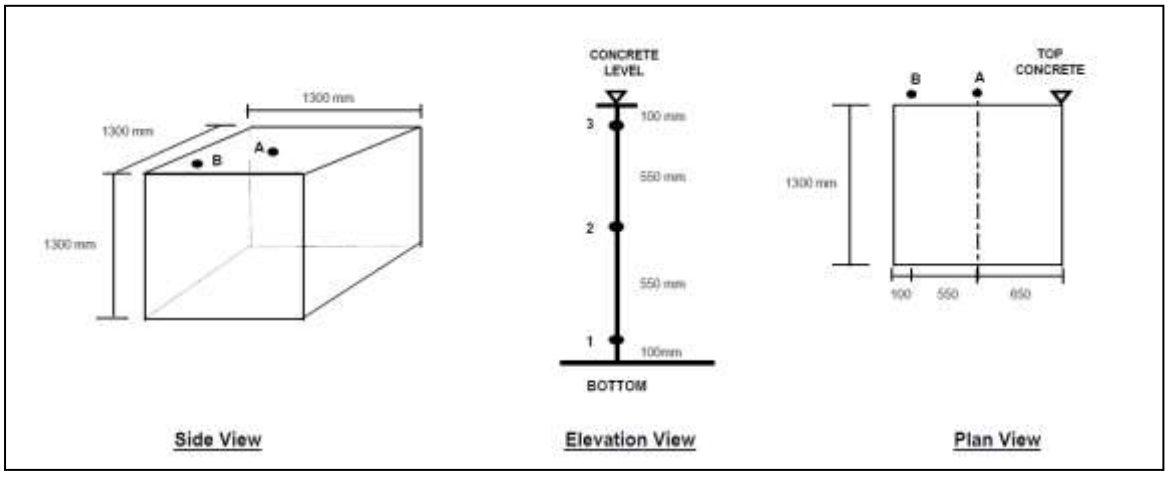

Figure 2. Sketch indicating locations of thermocouples in 1.3m x 1.3m x 1.3m hot-box for Stage 1-HB2

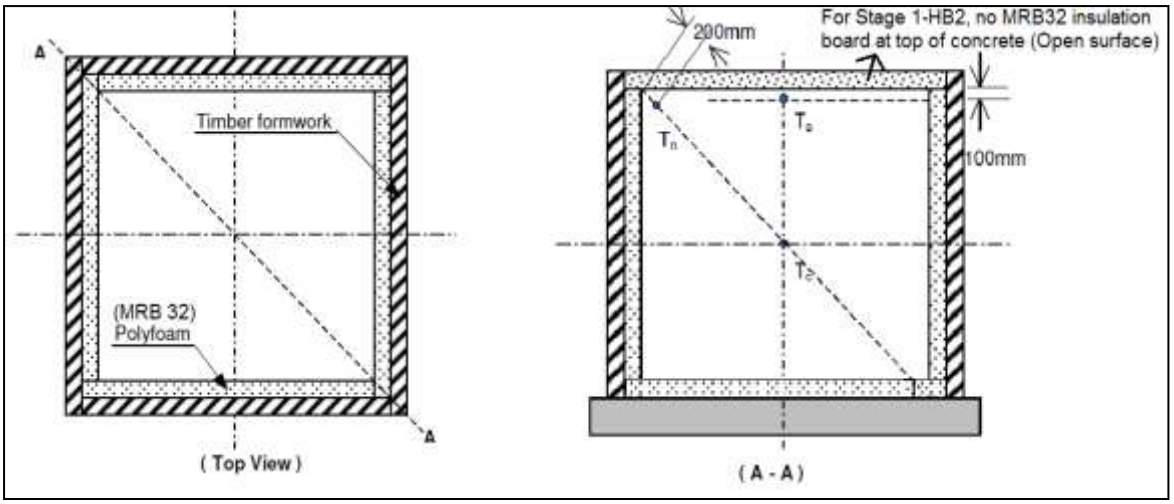

Figure 3. Sketch indicating locations of thermocouples in 1.5m x 1.5m x 1.5m hot boxes for Stage 1-HB1 & Stage 2-HB1 and 1.3m x 1.3m x 1.3m hot-box for Stage 1-HB2 (except top surface without insulation)

Table 6. Summary of concrete compressive strength, tensile strength and elastic modulus test results (Mass Concrete Class A, 2011)

	7Days			28Days			56Days		
Description	Stage 1-HB1 (2011)	Stage 2-HB1 (2012)	Δ	Stage 1-HB1 (2011)	Stage 2-HB1 (2012)	Δ	Stage 1-HB1 (2011)	Stage 2-HB1 (2012)	Δ
Compressive Strength (MPa)	25.25	23.43	1.82	33.05	31.77	1.28	38.15	39.77	1.62
Tensile Strength (MPa)	1.70	1.61	0.09	2.43	2.19	0.24	2.81	2.59	0.21
Modulus of Elasticity (MPa)	19.25	20.33	1.08	25.60	25.03	0.57	28.90	28.17	0.73

Based on the strength results shown in above Table 5, all concrete cubes tested at 7 days had exceeded the contract documents stipulated 90 days characteristic strength of 20MPa confirming that the required design strength of 20MPa is achievable within 28 day. Therefore, further optimization on content of cementitious material should be considered for lower heat of hydration.

Table 7. Summary of in-situ core test results (Mass Concrete Class A, 2011)

Description		FF1 50-200	FF1 500-650	FF1 50-200	FF1 500-650
	Unit	Aged 34 days		Aged 56 days	
Maximum load of failure	kN	667	643	741	687
Core compressive strength	MPa	37.7	36.4	41.9	38.9
In-situ compressive strength (as per BSEN 13791: 2007)	MPa	38.8	37.5	43.2	40.1
Cube compressive strength (see Table 6)	MPa	32.41		38.96	
Ratio of estimated in-situ cube strength to measured		1.20	1.16	1.10	1.03

In addition, internal cores were taken to study in-situ strength as shown in Figure 4. As expected with concrete containing flyash, the heat cycling had a beneficial effect on strength and the core strength is about 6.5 per cent higher comparing to the cube strength (see Table 7) measured at 56 days. The compressive strength test results confirm that the concrete is well above the specified requirements in terms of strength.

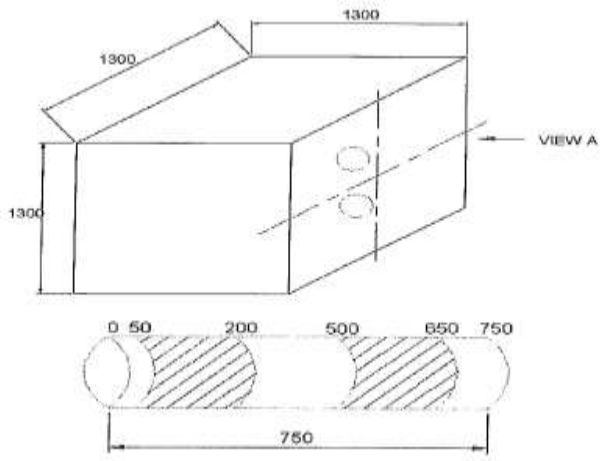

Figure 4. Sketch showing the in-situ strength with cores taken from 1.3m x 1.3m x 1.3m hot-box for Stage 1-HB2 (Mass Concrete Class A, 2011)

It was also observed that the differential for Stage-1 & Stage-2 strength tests at effective age of 7 days for the compressive strength, tensile strength and elastic modulus are 1.82 N/mm^2, 0.08 N/mm^2, and 1.08 N/mm^2 respectively.

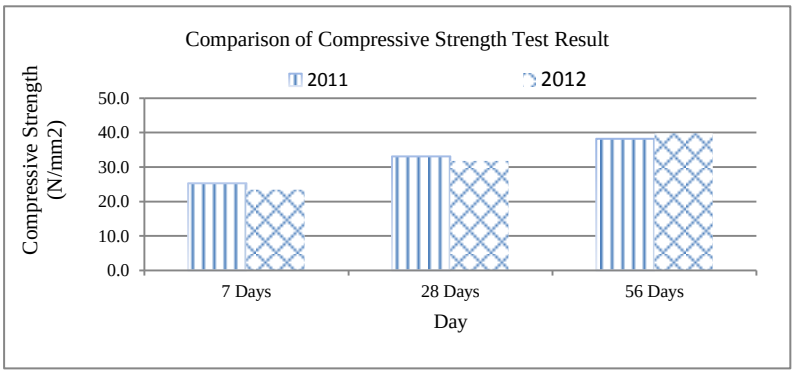

Figure 5. Comparison of compressive strength test results between Stage 1-HB1 and Stage 2-HB1 (Mass Concrete Class A, 2011)

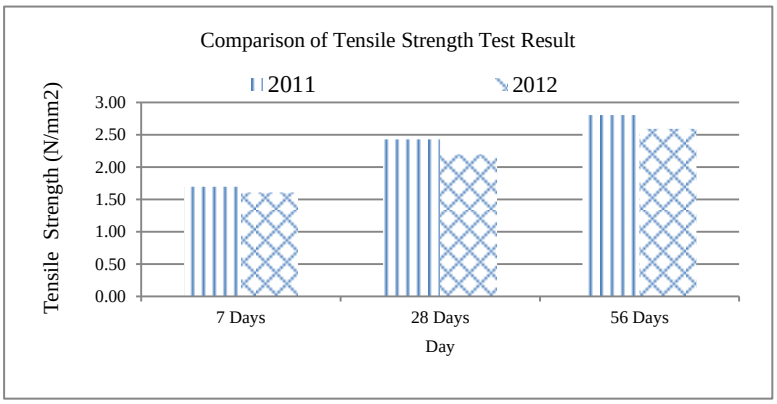

Figure 6. Comparison of tensile strength test results between Stage 1-HB1 and Stage 2-HB1 (Mass Concrete Class A, 2011)

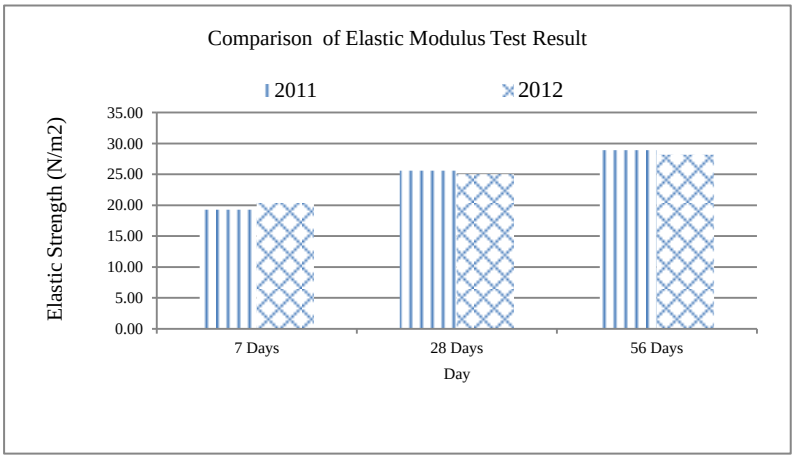

Figure 7. Comparison of elastic modulus test results between Stage 1-HB1 and Stage 2-HB1 (Mass Concrete Class A, 2011)

4. MODELLING OF ADIABATIC TEMPERATURE RISE

4.1 Modelled Heat Generation Curve using CIRIA C660 Formulas (Bamforth 2007)

CIRIA C660 formulas using British cementitious material is applied for modelling of heat generation curve basing on extensive study carried out in University of Dundee, United Kingdom. A two part two component equation for heat generation has been developed on this basis of the form:

Component 1 equation = the exponential curve, starting at time zero;

Component 2 equation = being delayed to start at time t2

The total heat generation for above two components, Q = Q1 + Q2, expressed in Equation 1, are presented below:

$$Q = Q_1 + Q_2 = \left[\left(\frac{Q_{ult}}{2}\right) \times \left(1 - e^{[(-B)\times(t^C)]}\right)\right] + \left[\left(\frac{Q_{ult}}{2}\right) \times \left(\frac{t-t_2}{t-t_2+D}\right)\right] \quad \text{(Eq.1)}$$

In order to establish values for the coefficients, analysis has been carried out on adiabatic test data from tests carried out at University of Dundee (Dhir et al. 2006) for cement with a start temperature of 20°C.

(a) Ultimate Heat Generation, Q41

Relationships between the CEM I and proportion of addition with flyash for the heat generated after 41 hours could be established basing on following expressions.

$Q41_{ult}$ (CEM I) = 351 kj/kg; Q41 (CEM I) = 330.11 kj/kg

Q41 (flyash) = Q41 (CEM I) - 2.989 * (%flyash) = 294.79 kj/kg

(b) Ultimate Heat Generation Qult

For flyash, Qult = Q41 (flyash) / (0.00002*(% flyash) ^2 - 0.0034 (% flyash) + 0.925)

(c) The Coefficient B

B = 0.011724, regardless of the cement type

(d) The Coefficient C

For flyash, C = 1.6-0.001*(% flyash)

(e) The coefficient D

For flyash, D = 6.2 + 0.2131 (% flyash)

(f) Activation time t2 for component 2

For fly ash, t2 = 3.5 + 0.0236(% flyash)

The constants and coefficients of heat generation for above item a), b), c), d), e) and f) are indicated in below Table 8.

Table 8. Constant & coefficient of heat generation of CEM II/B-V by method of CIRIA C660 (Bamforth 2007)

Constant	Unit	Value
% of Fly Ash	%	20
Q 41	kJ/kg	294.79
Q ult	kJ/kg	330.11
B	-	0.01172
C	-	1.59
D	-	8.331
t2	hrs	3.736

The modelled heat output (kj/kg) in the semi-adiabatic test and a Q_{ad} exponential curve measured at Q_{41} is 294.79 and 296.77 (See Figure 8b for exponential curve, Q_{ad}) respectively, which showing reasonably good correlation/ consistency has been obtained between prediction of temperature rise and the measured semi-adiabatic temperature rise derived from hot-box test, as graphically represented in below Figure 8a and 8b respectively.

4.2 Estimated Adiabatic Temperature Rise, Qad

The thermal model as provided in this paper uses the semi-adiabatic temperature rise data from published sources based on an extensive study carried out in University of Dundee, United Kingdom as the input. The hot-box tested as per the present trials was semi-adiabatic in nature as they are not perfectly insulated. This involves the establishment of different values of heat loss coefficient and adding incremental heat losses to the semi-adiabatic curve. A comparison between the estimated adiabatic curves is shown in below Figure 8a & 8b.

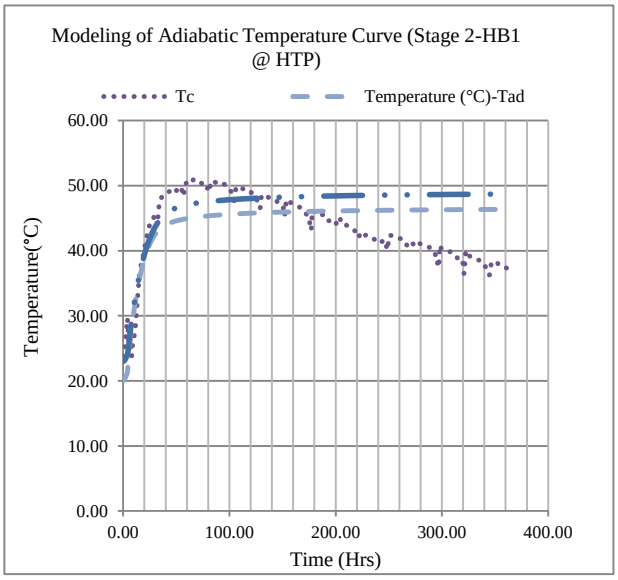

Figure 8a. Modelling of adiabatic temperature rise curve for CEMII-B-V by method of CIRIA (Bamforth 2007)

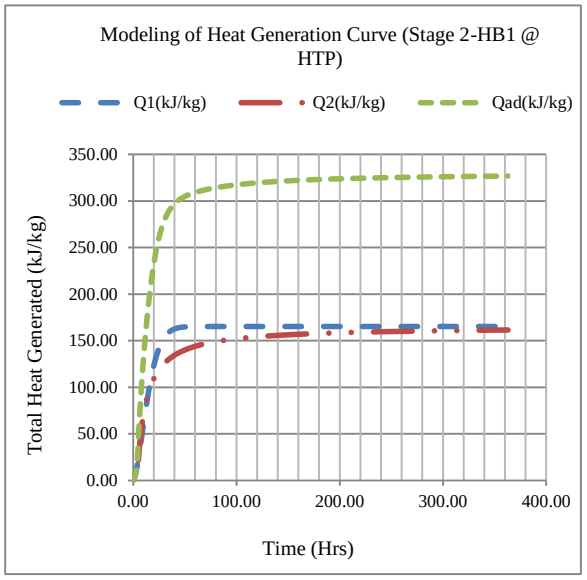

Figure 8b. Modelling of heat generation curve for CEMII-B-V by method of CIRIA 660 (Bamforth 2007)

The estimated maximum adiabatic temperature rise (MATR) measured at 72 hours is 23.72°C using data by method of CIRIA C660 could be used as input parameter for subsequent thermal modelling/ simulation i.e. heat of hydration analysis, from an initial placing temperature of 25°C. The aforesaid MATR could be further validated by using another empirical adiabatic hydration model (Tanabe et

al. 1985), as presented in below Equation 2, whereby the estimated MATR is 23.18°C, as detailed in Table 9.

$$Q(t) = Q_\infty \times (1 - e^{-\gamma t}) \quad \text{(Eq.2)}$$

Q_∞ = Ultimate adiabatic temperature rise,
γ = Constant on rate of temperature rise,
t = Age, in days
Q(t) = Adiabatic temperature rise at an age of t, in °C

The constant and coefficient of adiabatic heat generation using above Equation 2, is demonstrated in below Table 9.

Table 9. Constant & coefficients of heat generation of PFAC (Tanabe et al. 1985)

C	=	200	kg/m^3
t	=	3	days
Tp	=	20	°C

Table C15.3.1 Standard Value of Q

Type of cement	Placing Temperature Tp (°C)	Q(C) = AC+B A	B	Q_∞	$(1 - e^{-\gamma t})$
OPC	10	0.11	9.00	31.00	0.60
	20	0.10	10.00	30.00	0.89
	30	0.07	16.00	30.00	0.95
MHPC	10	0.10	4.00	24.00	
	20	0.08	11.00	27.00	0.78
	30	0.11	5.00	27.00	0.86
PFAC	20	0.13	-0.40	25.60	0.91

Table C15.3.2 Standard Value of γ

Type of cement	Placing Temperature T_p (°C)	Υ(C)= aC+b a (x 10^-3)	b	γ
OPC	10	0.0016	-0.017	0.303
	20	0.0016	0.409	0.729
	30	0.0037	0.273	1.013
MHPC	10	-	-	-
	20	2.40	0.032	0.512
	30	2.50	0.160	0.660
PFAC	20	0.20	0.746	0.786

Therefore, for PFAC:

$Q_{(t)}$	=	Q_∞ (1- e -γt)	
Q_∞	=	25.60	
$Q_{(t)}$	=	23.18	°C

Legend: (1) MHPC denotes Moderate Heat Portland Cement, (2) PFAC denotes Portland Fly Ash Cement (The blend ratio of flyash is 20%)

The standard values of Q and γ development calculations used are explained in detail in Standard Specification for Design and Construction of Concrete Structures, Part 2 Construction, Chapter 15: Mass Concrete (Page 141-142). Judging from the established values of 23.72°C and 23.18°C, it could be concluded that both prediction model has demonstrated good correlation in terms of adiabatic temperature rise of Portland flyash cement.

5. ADIABATIC TEMPERATURE RISE ANALYSIS AND INTERPRETATION OF RESULTS

5.1 Graphical Plots for Adiabatic Temperature Rise Monitoring Results (Adiabatic Temperature Rise Test Results 2011 & 2012)

From the adiabatic temperature rise monitoring test results (see Figure 9, 10 and 11), it could infer from VWSG's thermistor that the peak core temperature recorded for both phases of the trials i.e. Stage 1-HB1 @ point A2 (48.30°C) and Stage 2-HB1 (49.53°C) only showing minor differential of 1.53°C, whereby the established average peak core temperature is 48.915°C. This is well within the stipulated peak core temperature 50°C requirement.

a) Stage 1-HB1

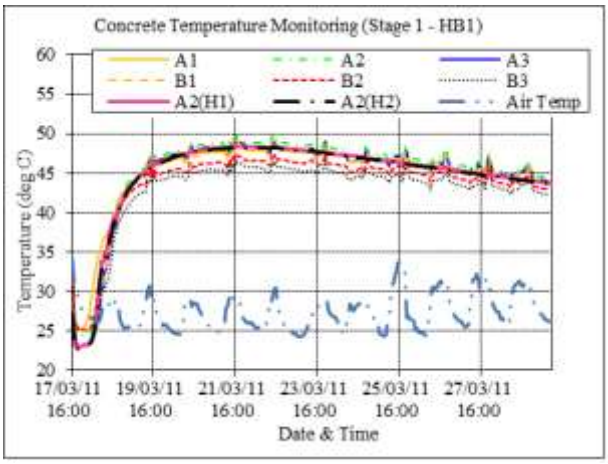

Figure 9. Experimental temperature rise data data for Stage 1-HB1

b) Stage 1- HB2

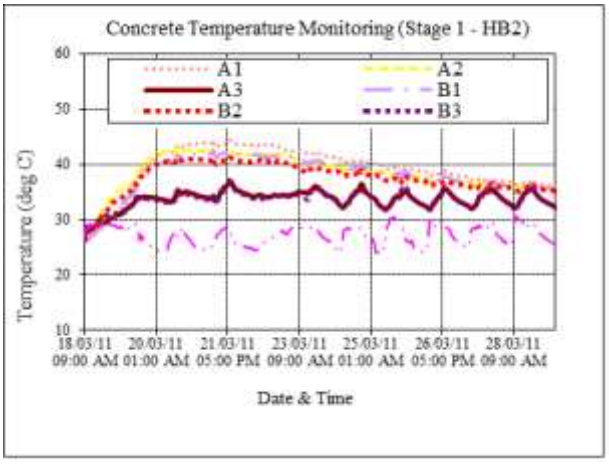

Figure 10. Experimental temperature rise for data for Stage 1-HB2

c) Stage 2-HB1

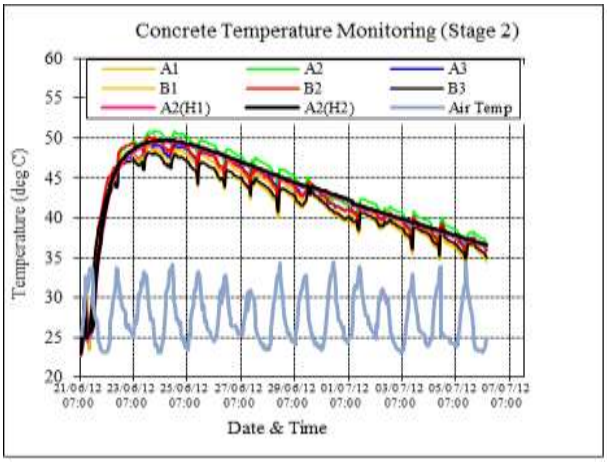

Figure 11. Experimental temperature rise data for Stage 2-HB1

The respective maximum temperature of T_c , T_n and its corresponding time of occurrence for Stage 1-HB1, Stage 1-HB2 and Stage 2-HB1 are summarised in below Table10.

Table 10: Comparison between peak temperature & time of occurrence

Stage	Peak Temperature at line A (°C) by VWSG			Peak Temperature at line B (°C) by thermocouples		
	Temp (°C)	Location	Time (Hrs)	Temp (°C)	Location	Time (Hrs)
1-HB1	48.30	A2 (Core)	1-HB1	48.30	A2 (Core)	1-HB1
1-HB2	44.43	A1 (Bottom)	1-HB2	44.43	A1 (Bottom)	1-HB2
2-HB1	49.53	A2 (Core)	2-HB1	49.53	A2 (Core)	2-HB1

Legend:
Line A located in center; Line B located at corner

T_c = Temperature at core, at Point A2 (center core)
T_s =Temperature at surface, at Point A1 (near bottom surface)
T_{cn} =Temperature at center, at Point B2 (at center)
T_n = Temperature at corner, at Point B1 (near top corner)

It has been demonstrated during mock-up test (Test Report for Mass Concrete, 2013); the core reaches its maximum temperature in about 72 hours after concrete placement.

5.2 Effects of Size of Concrete Block and Boundary Condition

The maximum temperature at center heavily depends on the insulation and the size of the hot-block. The results indicate that the center of a 1.5m x 1.5m x 1.5m mass concrete hot-box with proper insulation could produce the maximum core temperature T_c very close to that under full adiabatic condition. This implies that the maximum temperature at the center of a concrete block is little affected by the size of the concrete if the dimension is big enough.

The adiabatic temperature rise test simulation by method of CIRIA C660 (using identical mix design and input parameter as indicated in below *Table 11*) showing that hot-box size of 3m x 3m x 3m and greater having proper 50mm thick polyfoam insulation will yielded Tc at full adiabatic temperature. Furthermore, for a concrete hot-box of dimension 4m x 4m x 4m, the temperature recorded has exhibited full-adiabatic behaviour even without any insulation as the block size is big enough. However, this is non-practical for any laboratory mock-up test to be considered in such huge block dimension unless it is cast in-situ for thick raft foundation.

Table 11. Input parameters for thermal simulation

Item	Description	Value	Unit
I	Input Parameters - Concrete		
	Type of cement	CEM II:B-V	
	Binder content	200	kg/m^3
	Aggregate type	Granite	
	Density	2380	kg/m^3
	Pour thickness	1.5	m
	Insulation	0.05	m
	Insulation removal	168	hours
II	Input Parameters - Environment		
	Concrete placing temperature	25	°C
	Ambient temperature (mean)	27	°C
III	Input Parameters - Heat Exchange		
	Surface conductance	1.30	W/m^2.K
	Concrete thermal conductivity	3.028	W/m.K
	Concrete specific heat	1.037	kJ/kg.°C
	Thermal diffusivity	0.0051	m^2/h

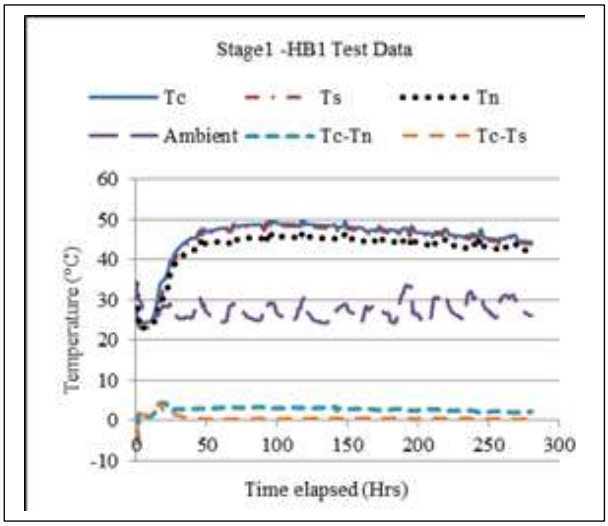

Figure 12. Temperature rise curve and differential in 1.5m x 1.5m x 1.5m hot box for Stage 1-HB1

Figure 12 presents the maximum temperature difference of (T_c – T_n) and (T_c – T_s) in a 1.5m x 1.5 x 1.5m concrete hot-box. The results reveal that the effective insulation using polyfoam of low conductance material plays a dominant role in controlling the maximum temperature difference across the block, even though the core temperature varies marginally.

Referring to below Table 12, for 1.5m x 1.5m x 1.5m hot box tests (Stage 1-HB1 and Stage 2-HB1), the adiabatic temperature rise differential of 1.23°C (49.53°C minus 48.30°C) at center is little affected by the environment due to good insulation on concrete blocks; while the temperature

differentials ($T_c - T_n$) and ($T_c - T_s$) are affected to some degree between 1.79°C to 4.53°C. Whereby the recorded maximum temperature differentials between ($T_c - T_n$) and ($T_c - T_s$) are 4.66°C and 4.53°C respectively. As for the case of 1.3m x 1.3m x 1.3m hot box (Stage 1-HB2), the direct exposure of concrete surface to air is measured whereby the recorded maximum temperature differential between ($T_c - T_n$) and ($T_c - T_s$) is 9.22°C and 8.88°C respectively, which was about two-fold than the fully insulated hot block as in the case of 1.5m x 1.5m x 1.5m hot box. Therefore, direct exposure of concrete surface to air or the use of steel formwork would expect even higher temperature differentials for ($T_c - T_n$) and ($T_c - T_s$).

Table 12. Maximum T_c, $T_c - T_n$ and $T_c - T_s$

Stage	Stage 1-HB1		Stage 1-HB2		Stage 2-HB1	
	Temperature (°C)	Time (Hrs)	Temperature (°C)	Time (Hrs)	Temperature (°C)	Time (Hrs)
Peak T_c (°C)	48.30	96	42.81	72	49.53	66
Peak (T_c - T_n) (°C)	4.46	19	9.22	47	3.14	56
Peak (T_c - T_s) (°C)	4.53	17	8.88	47	1.79	76

Legend:
T_c =Temperature at core, at Point A2 (center core)
T_s = Temperature at surface, at Point A3 (near top surface)
T_n = Temperature at corner, at Point B3 (near top corner)

5.3 Temperature Rise and Temperature Distribution for Stage 1 & Stage 2 Hot-Box Tests
The two hot-box trials have exhibited slightly different rates of temperature rise at some period during the experiments, whereby their peak core temperature rise values recorded by thermistors (strain gauges) only differed by around 1.225°C as shown in below Table 13. Likewise the difference in peak core temperature recorded by thermocouples is 1.25°C as shown in Table 14.

The differences in aforesaid peak core temperatures could be attributed to lower initial concrete placing temperature for Stage 1: HB1 hot box (average 23°C) as compare to Stage 2: HB1 hot box (average 25°C). This slight difference in temperature rise rate was also attributed to the rate of heat gain during phase 2 (Stage 2- HB1) is faster, resulting from different fineness and age of cement used during phase-1 and phase-2 test resulting in different rate of hydration.

Table 13. Summary of Test Results for Peak Core Temperature @ A2 recorded by Strain Gauges

Hot-Block	Stage 1-HB1 (°C)	Stage 2-HB1(°C)	Difference (°C)
Strain Gauge No.1 (°C)	48.3	49.34	-
Strain Gauge No.2 (°C)	48.24	49.65	-
Average (°C)	48.27	49.495	1.225

Table 14. Summary of Test Results for Peak Core Temperature @ A2 & B2 recorded by Thermocouples

Hot-Block	Stage 1-HB1 (°C)	Stage 2-HB1 (°C)	Difference (°C)
Thermocouple @ A2 (°C)	49.69	50.94	1.25
Thermocouple @ B2 (°C)	49.26	50.22	-
Average (°C)	49.475	50.58	1.105

The various temperature rise curves, temperature differentials, and temperature distribution profiles are shown in Figures 12-16. Due to the greater heat loss rate at corner and side of the block, the temperatures at corner and side reach the peak before the maximum core temperature due to heat exchange to the environment. The center temperature begins to decrease when the heat generated in block is not enough to compensate the heat loss to the environment (as for the case of adiabatic condition). After the decrease of the core temperature, the temperature difference ($T_c - T_n$) and ($T_c - T_s$) gradually climb to the peak. This is normally regarded as the critical period for the surface

concrete. Situations would become even worse if the formwork is removed during this stage. Also, the poor insulation could significantly reduce the time to reach the maximum temperature differences of ($T_c - T_n$) and ($T_c - T_s$). This infers that poorly insulated mass concrete could develop thermal cracks shortly after the placement.

The temperature at center is little affected by the environment variation due to the good insulation and big enough size of the hot box i.e. 1.5m x 1.5m x 1.5m, while the temperature difference ($T_c - T_n$) and ($T_c - T_s$) is affected in some degree. Essentially, during the course of insulation selection, it is necessary to consider the environment heat loss variation to minimize the effect. It is thus inferred that temperature gradient of actual concrete structures could be improved by additional insulation at edges and corners. The temperature gradient along the regions close to the side is much steeper than that in the central region. This suggests that the locations of the thermocouples in the concrete mock-up block should be carefully defined so that the comparable results can be obtained.

Figures 12-14 showing how the temperature gradients formed after the concrete were cast into hot box. Temperature differential formed from the very beginning of the temperature rise in the concrete mass, whereby the temperature is also affected by the ambient temperature fluctuation, which is formed by the temperature change from daytime to night-time. The peak value of ($T_c - T_n$) and ($T_c - T_s$) occurred after T_c.

This implies that the maximum temperature difference was encountered in the cooling down period of the concrete mass. The temperature differences of between centre core versus surface ($T_c - T_s$) and between core versus corner ($T_c - T_n$) were also demonstrated in below Figure 15 and Figure 16, which showing how the temperature at the corner of the block had the lowest value while the temperature at center gave the highest. ($T_c - T_n$) is always greater than ($T_c - T_s$). This may be explained as that the heat loss in the corner of the block is multi-dimensional. The peak value of ($T_c - T_n$) and ($T_c - T_s$) occurred after T_c.

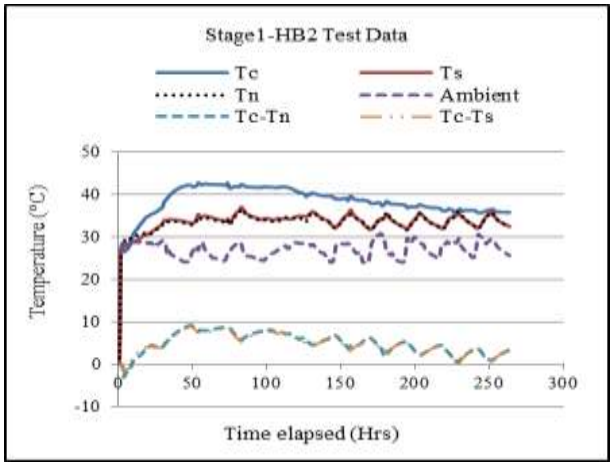

Figure 13. Temperature rise curve and temperature differential in 1.3 x1.3x1.3m hot-box for Stage 1-HB2

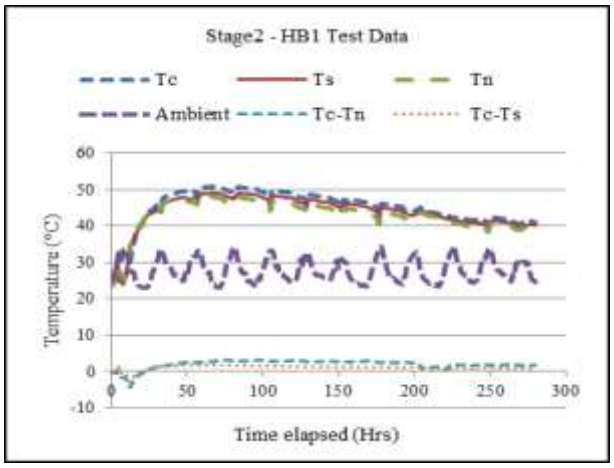

Figure14. Temperature rise curve and temperature differential in 1.5x1.5 x 1.5m hot-box for Stage 2-HB1

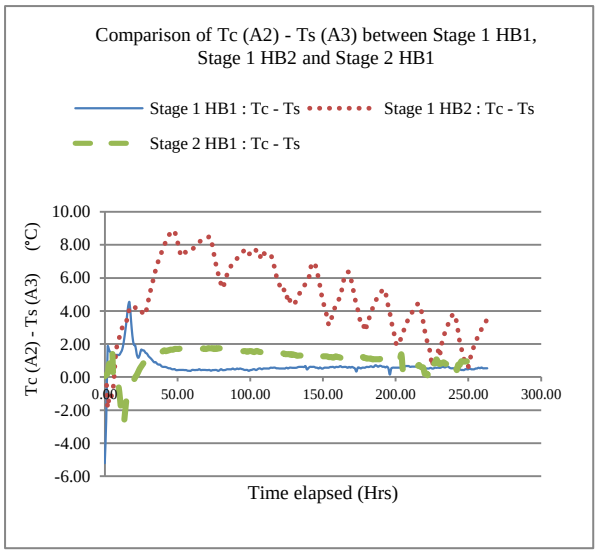
Comparison of Tc (A2) - Ts (A3) between Stage 1 HB1, Stage 1 HB2 and Stage 2 HB1
Stage 1 HB1 : Tc - Ts
Stage 1 HB2 : Tc - Ts
Stage 2 HB1 : Tc - Ts
Tc (A2) - Ts (A3) (°C)
Time elapsed (Hrs)

Figure 15. Comparison of temperature differential between Tc-Ts for Stage 1-HB1, Stage 1-HB2, and Stage 2-HB1

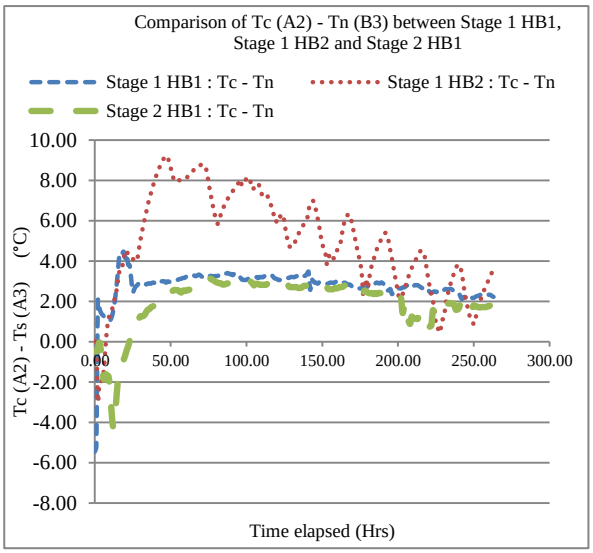
Comparison of Tc (A2) - Tn (B3) between Stage 1 HB1, Stage 1 HB2 and Stage 2 HB1
Stage 1 HB1 : Tc - Tn
Stage 1 HB2 : Tc - Tn
Stage 2 HB1 : Tc - Tn
Tc (A2) - Ts (A3) (°C)
Time elapsed (Hrs)

Figure 16. Comparison of temperature differential between Tc-Tn for Stage 1-HB1 and Stage 2-HB1

5.4 Temperature differential

The maximum differential temperature (Temperature recorded at point A1 minus temperature recorded at point A3) for stage 1-HB2 at the open top surface was found to be ~ 10.13°C, measured on 21st March 2011 at 09:00 am, about 72 hrs after the concrete placement. The top thermocouple was located 100mm below the surface. However an adjustment is required to determine the true differential between the centre and the surface. This adjustment is made by assuming the temperature profile follows a parabolic curve to the cooling surface as shown in Figure 17. With a peak temperature of 44.43°C as recorded, the difference between the surface and the point of location of the thermocouple at 100mm depth is about 2.3°C. This must therefore be added to the measured differential. Hence the true differential is 10.13 + 2.3 = 12.43°C ≈ 12.5°C. This is significantly less than the Contract Documents specified 20°C and the proposed differential of 27.7°C for granite aggregate concrete as in accordance with BS8110-2: 1985, Table 3.2- Estimated limiting temperature changes to avoid cracking.

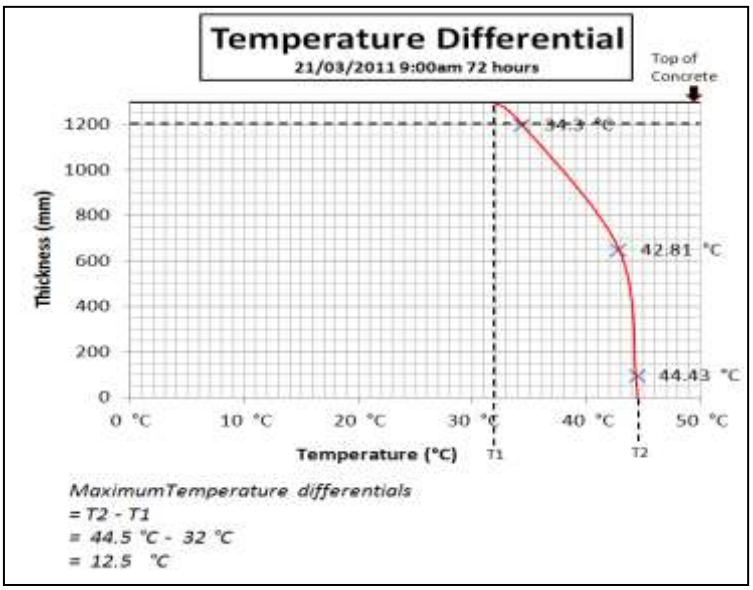

Figure 17. Adjustment for temperature differential at top surface of 1.3m x 1.3m x 1.3m hot-box, Stage 1- HB2

6. DISCUSSIONS

1. The two hot-box trials have exhibited slightly different rates of temperature rise at some period during the experiments, whereby their peak core temperature rise values differed by merely 1.225°C only. The difference in peak core temperature could be attributed to lower initial concrete placing temperature for Stage 1: HB1 hot-box (average 23°C) as compare to Stage 2: HB1 hot-box (average 25°C). This slight difference in temperature rise rates may be attributed to the rate of heat gain during Phase 2 (Stage 2- HB1) is faster, which could be further attributed to different fineness and age of cement used during Phase-1 and Phase-2 test resulting in different rate of hydration.
2. From the two experiments performed, the difference in peak core temperature rise for both trials was merely 1.225°C and 1.25°C, as recorded by strain gauges (built-in thermistor) and thermocouples respectively. This implies that the concrete temperature during the entire duration of the tests varying only by a small amount.
3. As expected with concrete containing flyash, cores extracted from Stage 1-HB2 demonstrated that the in-situ heat cycles had a beneficial effect on fly-ash concrete, with the average estimated in-situ strength being about 6.5 per cent higher than the test cube strength at 56 days. This compressive strength results confirm that the proposed flyash concrete is well above the specified requirements in terms of strength and hence compliance with the technical specification requirements.
4. The computer thermal modelling/ simulation revealed that for a concrete hot-box of dimension 2.5m x 2.5m x 2.5m coupled with good insulation (50mm thick polyfoam), the maximum core temperature recorded by thermal probe is almost near full-adiabatic state whereby no loss of heat to the environment. Likewise for a concrete hot-box of dimension 4m x 4m x 4m, the temperature recorded has exhibited full-adiabatic behaviour without any insulation as the block size is big enough. However, this is non-practical both technically and commercially for any laboratory mock-up test to be considered in such huge block dimension unless it is cast in-situ for thick raft foundation.

7. CONCLUSIONS

1. From the adiabatic temperature rise monitoring test, it could infer from strain gauges that the peak temperature values recorded for both phases of the trials i.e. Stage 1-HB1 (48.30°C) and Stage 2-HB2 (49.53°C) is merely difference by 1.23°C, whereby the established average peak core temperature and maximum core-surface differential was 49.53°C and 12.5°C (worst case scenario for Stage 1-HB2) respectively are well within stipulated 50°C and 20°C requirements as specified in various project technical specifications, from a maximum initial placing temperature of 25°C. As demonstrated during mock-up test that the core reaches its maximum temperature in about 72 hours after concrete placement.
2. Significant reduction of temperature rise and maximum temperature rise rate of PFAC concrete under adiabatic condition was successfully demonstrated in this experimental investigation. This indicates that the application of CEM II/B-V cement is effective and beneficial in mass concrete pours in minimizing the mass overheating inducing thermal cracking. Thus the use of flyash as partial replacement for Portland cement resulted in lower adiabatic temperature rise.
3. The outcome of the hot-box test suggests that good insulation is critical in minimising the temperature difference in mass concrete. In mass concrete pouring, additional insulation at edges and corners can help to improve temperature gradient in the critical regions. Moreover, hasty removal of the formwork during the concrete cooling down period may greatly increase the temperature gradient, and this could be detrimental to the surface of concrete mass.

4. All concrete cubes compressive strength results tested at 7 days had exceeded the contract documents stipulated 90 days characteristic strength of 20MPa confirming the compliance of proposed 20MPa concrete mix design.
5. Both empirical adiabatic hydration models (CIRIA C660, 2007 and Tanabe et al. 1985) have demonstrated good agreement on the maximum adiabatic temperature rise values of 23.72°C and 23.18°C respectively. Thus, the heat of hydration model by method of CIRIA C660 can be successfully used in modelling the characteristics of semi-adiabatic temperature rise data of 20MPa mass concrete adopted in this study.
6. As far as the determined adiabatic temperature rise monitoring results is concern, the established results could be inferred for in-situ thermal properties of 20MPa mass concrete application, as the results could be repeatable on account of similar types of constituent materials and concrete mix design adopted for permanent works at project site.

References

[1] ACI Committee 207.2R-07, 2007. Report on Thermal and Volume Change Effects on Cracking of Mass Concrete. Reference.
[2] ACI Committee 305.1-06, 2007. Specification for Hot Weather Concreting.
[3] ACI Committee 207.1R-96, 1996. Specification for Mass Concrete.
[4] Adiabatic Temperature Rise Test Result (from 17/3/2011 to 29/3/2011), Stage 1, for 265MW TNB Hulu Terengganu Hydroelectric Project, Malaysia.
[5] Adiabatic Temperature Rise Test Result (from 21/6/2012 to 6/7/2012), Stage 2 for 265MW TNB Hulu Terengganu Hydroelectric Project, Malaysia.
[6] Bamforth P. B. 2007. CIRIA C660 Early-Age Thermal Crack Control in Concrete, CIRIA, London.
[7] BS 8110-2: 1985, Structural Use of Concrete – Part 2: Code of Practice for Special Circumstances. BSI, London.
[8] BS EN 13791: 2007, Assessment of In-situ Compressive Strength in Structures and Precast Concrete Components. BSI, London.
[9] BS EN 196-9: 2010, Methods of Testing Cement. Heat of Hydration. Semi-Adiabatic Method, BSI, London.
[10] CIMA Cement Test Certificates on NS Ecocrete-LH, CEM II/ B-V 42.5N-LH (January 2011 and June 2012), CIMA, Malaysia.
[11] DD ENV 206:1992, Concrete: Performance, Production, Placing and Compliance Criteria, BSI, London.
[12] Guo D S et al. 2001. Experimental Modeling of Temperature Rise of Mass Concrete by FDM Method, 26th Conference on Our World in Concrete & Structures, 27-28 August 2001. Singapore.
[13] Japan Society of Civil Engineers (JSCE), Standard Specification For Design And Construction Of Concrete Structures (First Edition 1986), Part 2 (Construction), Chapter 15: mass Concrete, 141-142, Tokyo, Japan.
[14] Lee MH, Khil BS, and Yun HD 2014. Influence of Cement Type on Heat of Hydration and Temperature Rise of Mass Concrete (Accepted 9 June 2014).
[15] Mass concrete Class A/Grade III Concrete Mix Trials and Hot Block Monitoring, Overview of Results, Report 1202/11/7322, (2011) for 265MW TNB Hulu Terengganu Hydroelectric Project, Malaysia.
[16] MS 523-2: 2011, Concrete – Part 2: Method of Specifying and Guidance For The Specifier (Second Revision), Department of Standards Malaysia, Malaysia.
[17] Neville, A.M., Brooks, J.J., Advanced Concrete Technology (Second Edition 2010), Chapter 9: Temperature Problems in Concreting, 161-168, Publisher, London.
[18] Tanabe T, Kawasumi M and Yamashita M. Thermal Stress Analysis of Massive Concrete: Finite Element Analysis of the Reinforced Concrete Structures, (ASCE), 1985, 407-421.

[19] Technical Specification (Jan 2000) [Gutteridge Haskins & Davey (GHD)] for Construction of Sg. Kinta Dam and Associated Works, Section 10, Clause 10.2.9.
[20] Technical Specification (2007) [Sepakat Setia Perunding (SSP)] for Construction and Completion of Sg. Batu Hampar Dam and Associated Works, Section 10: Clause 10.2.9.
[21] Technical Specification (2009) [SMEC International] for Lot CW2 – Main Civil and Associated Works, Volume 3: Part 1 of 2, Section 9: RCC, Section 10: Clause 10.10.1 & Section 11: Clause 11.2 – Concrete Production and Construction.
[22] Technical Specification (2010) [SMEC International] for Lot CW2 – Main Civil and Associated Works, Volume 3: Part 1 of 2, Section 10: Clause 10.10.1 & Section 11: Clause 11.2 – Concrete Production and Construction.
[23] Technical Specification (2013) [SNC–Lavalin Power] for Chenderoh Unit 5 Hydroelectric Project, Section 7.3.3.: Clause 4 & 5.
[24] Test Report for Determination of Heat of Hydration on Portland Cement at & Days using BS EN 196-8: 2003, Ref.: CT-16925/JAS dated 25/07/2011.
[25] Test Report for Mass Concrete Temperature Monitoring for Mock-up of 1.5m x 1.5m x 1.5m Hot Box (2013), Report No.: TEM 003/12/R0855 for 265MW TNB Hulu Terengganu Hydroelectric Project, Malaysia